Official Journal of the World Federation
for Ultrasound Medicine and Biology

# Ultrasound
## in medicine and biology

Volume 37, Number 9, September 2011

Clinical Applications

Biophysics and Bioeffects

Transducers and Signal Processing

Therapeutic Applications

ELSEVIER
ISSN: 0301-5629

View the journal at www.umbjournal.org

**ELSEVIER**

● *Original Contribution*

# NONINVASIVE *IN VIVO* LIVER FIBROSIS EVALUATION USING SUPERSONIC SHEAR IMAGING: A CLINICAL STUDY ON 113 HEPATITIS C VIRUS PATIENTS

ÉRIC BAVU,*¶ JEAN-LUC GENNISSON,* MATHIEU COUADE,† JEREMY BERCOFF,† VINCENT MALLET,‡
MATHIAS FINK,* ANNE BADEL,§ ANAÏS VALLET-PICHARD,‡ BERTRAND NALPAS,‡
MICKAËL TANTER,* and STANISLAS POL‡

*Institut Langevin - Ondes et Images, ESPCI ParisTech (UMR CNRS 7587/INSERM U979), Paris, France; †Supersonic
Imagine, Aix-en-Provence, France; ‡Unité d'hepatologie, (INSERM U567), Hopital Cochin, Universite Paris Descartes, Paris,
France; §Équipe Bioinformatique génomique et moléculaire, (INSERM UMRS 726) Paris, France; and ¶Laboratoire de
Mécanique des Structures et des Systèmes Couplés, Conservatoire National des Arts et Métiers (EA 3196), Paris, France

**Abstract**—Supersonic shear imaging (SSI) has recently been demonstrated to be a repeatable and reproducible
transient bidimensional elastography technique. We report a prospective clinical evaluation of the performances
of SSI for liver fibrosis evaluation in 113 patients with hepatitis C virus (HCV) and a comparison with FibroScan
(FS). Liver elasticity values using SSI and FS ranged from 4.50 kPa to 33.96 kPa and from 2.60 kPa to 46.50 kPa,
respectively. Analysis of variance (ANOVA) shows a good agreement between fibrosis staging and elasticity assess-
ment using SSI and FS ($p < 10^{-5}$). The areas under receiver operating characteristic (ROC) curves for elasticity
values assessed from SSI were 0.948, 0.962 and 0.968 for patients with predicted fibrosis levels $F \geq 2$, $F \geq 3$ and
$F = 4$, respectively. These values are compared with FS area under the receiver operating characteristic curve
(AUROC) of 0.846, 0.857 and 0.940, respectively. This comparison between ROC curves is particularly significant
for mild and intermediate fibrosis levels. SSI appears to be a fast, simple and reliable method for noninvasive liver
fibrosis evaluation. (E-mail: eric.bavu@espci.fr)    © 2011 World Federation for Ultrasound in Medicine &
Biology.

*Key Words:* 2-D transient elastography, Shear wave imaging, Shear wave spectroscopy, Ultrasound, Liver fibrosis
staging.

## INTRODUCTION

Liver fibrosis, which results from persistent hepatic
inflammation, has serious long-term consequences for
patient morbidity and mortality in relation to cirrhosis
evolution (World Health Organization 2004). As a conse-
quence, the assessment of liver fibrosis is of crucial
clinical importance for the diagnosis and monitoring of
chronic liver diseases at early stages (Beaugrand 2006)
and treatment monitoring (Pinzani et al. 2005).

Liver biopsy (LB) is still considered as the "gold
standard" examination to assess the liver fibrosis level,
despite limitations (Afdahl 2003), such as patient refusal,
patient discomfort, morbidity and even mortality (Cadranel
et al. 2000; Friedman 2003; Castéra et al. 1999; Bravo et al.
2001). The specificity and sensitivity of LB has also

been questioned (Beaugrand 2006; Bedossa et al. 2003;
The French METAVIR Cooperative Study Group 1994;
Colloredo et al. 2003) because of the intraobserver and
interobserver variability of the examination (Maharaj
et al. 1986). These variabilities can be explained by
sampling errors during punctures (Maharaj et al. (1986);
Regev et al. (2002), fibrosis heterogeneities in the liver
tissues and accentuated by the small length of liver
samples (Maharaj et al. 1986; Ziol et al. 2005).

Such limitations led to the development of surrogate
serum markers and noninvasive biochemical such as
glycomics, fibrotest, fibrometer, hepascore, aspartate
transaminase to platelet ratio (APRI), Fib 4 or Forn's
score and morphologic tests such as FibroScan (FS,
Echosens, Paris, France) (Trinchet 1995; Halfon et al.
2005; Wai et al. 2003; Forns et al. 2002; Imbert-Bismut
et al. 2001; Ono et al. 1999; Sterling et al. 2006;
Vallet-Pichard et al. 2007). Several studies reported
that the combination of different blood markers and the
assessment of tissue elasticity based on transient

---

Address correspondence to: Éric Bavu, Institut Langevin - Ondes
et Images, ESPCI ParisTech (UMR CNRS 7587/INSERM U979), 10,
rue Vauquelin, 75005, Paris, France. E-mail: eric.bavu@espci.fr

elastography by FibroScan (FS) has shown good results in liver fibrosis staging (Ziol et al. 2005; Fontana and Lok 2002; Lackner et al. 2005; Castéra et al. 2005). Although being used in conjunction with FS, those blood indexes are reported to be not specific enough (Beaugrand 2006; Bataller and Brenner 2005; Stauber and Lackner (2007) and could be influenced by extrahepatic diseases including hemolysis. Furthermore, the most important limitation of these fibrosis tests is the bad discrimination between intermediate stages of fibrosis (Stauber and Lackner 2007; Parkes et al. 2006). As a consequence, there is a critical need for alternative fibrosis methods for liver fibrosis staging allowing high specificity and sensibility (Friedman 2003; Stauber and Lackner 2007) for intermediate more than for advanced stages of liver fibrosis to initiate treatments.

Elasticity imaging (Ophir et al. 1991; Sarvazyan et al. 1998) is now widely considered as a useful technique for biologic tissues characterization. Recently, several elasticity imaging techniques have been developed for the assessment of the mechanical properties of liver tissues (Yeh et al. 2002) and fibrosis level staging, using different imaging modalities, such as magnetic resonance elastography (Klatt et al. 2006); Muthupillai et al. 1995; Huwart et al. 2008), two-dimensional (2-D) static ultrasound elastography (Friedrich-Rust et al. 2007), one-dimensional (1-D) transient ultrasound elastography (Sandrin et al. (2003), supersonic shear imaging (SSI) (Muller et al. 2009), shearwave dispersion ultrasound vibrometry (SDUV) (Chen et al. 2009), spatially modulated ultrasound radiation force (SMURF) imaging (McAleavey et al. 2009), sonoelastography (Taylor et al. 2000) and acoustic radiation force impulse (ARFI imaging) (Fahey et al. 2008; Palmeri et al. 2008; Yoneda et al. 2010), which is already commercially implemented by Siemens company. All these methods are based on the same methodology: the liver is mechanically stressed and the induced tissue displacement in the organ is measured, allowing the estimation of the elastic properties in the liver, which are known to be related to the degree of hepatic fibrosis. Some of the procedures involve a static compression of the liver and do not allow quantitative estimation of the liver stiffness (Friedrich-Rust et al. 2007).

Supersonic shear imaging was already evaluated in the framework of breast cancer diagnosis (Athanasiou et al. 2010), muscular (Gennisson et al. 2010) and cornea (Tanter et al. (2009) stiffness assessments. In a recent paper (Muller et al. 2009), Muller et al. presented a feasibility study of the SSI and shear wave spectroscopy (SWS) for the quantitative mapping of human liver using a linear ultrasonic probe. This imaging technique is based on the combination of the acoustic radiation force imaging technique and an ultrafast echographic imaging approach,

allowing the assessment a quantitative elasticity map of biological tissues in a single ultrasonic sequence (Muller et al. 2009; Bercoff et al. 2004a, 2004b; Tanter et al. 2008). This preliminary *in vivo* feasibility on 15 healthy volunteers (Muller et al. 2009) showed that the SSI technique is promising and that the liver stiffness estimation on a large area ($10 \, cm^2$) using the SSI mode is fast (less than 1 s), repeatable (5.7% standard deviation) and reproducible (6.7% standard deviation). Moreover, it was shown in (Muller et al. 2009) that both elasticity and viscosity can be assessed using SSI. In many organs, tissue exhibit shear viscosity and signal processing of the shear wave propagation movie can be refined to study this more complex biomechanical behavior. Viscosity affects the shear wave propagation speed (Bercoff et al. 2004c; Deffieux et al. 2009). The time profile of the plane shear wave is progressively distorted and attenuated during propagation. This distortion is characterized by a frequency dependence of the shear wave speed and attenuation that fully describes the rheologic behavior of tissue (Deffieux et al. 2009) as already shown in breast cancer diagnosis (Tanter et al. 2008). Simple signal processing on acquired data enables to provide the dispersion curve of the shear wave phased speed.

The purpose of our clinical study was to determine the efficiency of this method for liver fibrosis level evaluation and prospectively compare the sensitivity and specificity of SSI with those of the FS for hepatic fibrosis levels in patients with hepatitis C virus (HCV). Our results demonstrate that SSI is feasible and appear to be at least as efficient as FS for intermediate levels.

## MATERIAL AND METHODS

### Patients

Between June 2008 and June 2009, a cohort of 113 consecutive patients participated in the study after giving their informed consent. Each patient underwent on the same day FS, SSI elasticity mapping and surrogate blood tests in the hepatology department of Cochin Hospital (Paris France) between June 2008 and June 2009, because they had established Hepatitis C virus and were not under treatment. This study has been approved by the French National Committee for the Protection of Patients Participating in Biomedical Research Programs (Comité de Protection des Personnes CPP Ile de France III No. 08003) and by the ethics committee of the Cochin Hospital. This study includes 53 men and 60 women, from 21 to 84-years-old (mean age 55 years, standard deviation 12 years), with a mean body index of 24.0 $kg.m^{-2}$ (standard deviation: 3.8 $kg.m^{-2}$). Two patients (1.76%) were excluded from the statistical analysis because of unreliable or impossible FibroScan measurement (both were overweight or obese). Three patients (2.65%) were

excluded because of unreliable SSI measurement (no successful reproducibility, one patient was overweight or obese). The 108 patients included in the statistical study were classified following a predicted fibrosis score that was based on the concordance analysis of surrogate serum markers and liver biopsy (when available, *i.e.*, for 39 patients) on a METAVIR fibrosis scale (Bedossa and Poynard 1996) from 0 to 4 (4 corresponding to cirrhosis). Fifty, 19, 24 and 15 patients have fibrosis $F_{0-1}$, $F_2$, $F_3$ and $F_4$, respectively.

*Surrogate serum markers*

The following parameters were determined from blood samples at Hopital Cochin the same day that the FS examination was performed: aspartate transaminase level (AST), alanine transaminase level (ALT), $\gamma$ glutamyl transferase level (GGT), cholesterol and platelets count. The aspartate transaminase to platelets radio index (APRI) (Wai et al. 2003) is calculated as:

$$APRI = \frac{AST[IU/L]/\text{Upper limit of normal }[IU/L]}{\text{platelet count}\left[10^9/L\right]} \times 100$$

(1)

An APRI value $>2.10$ is associated with a positive predictive value (PPV) and a negative predictive value (NPV) for cirrhosis of 65% and 95%, respectively. An APRI value $<0.50$ has a PPV and a NPV for significant-fibrosis ($F_{2-4}$) of 61% and 86%, respectively. An APRI value $\leq 1.00$ has a PPV and a NPV for cirrhosis of 35% and 100%, respectively. An APRI value $\leq 1.50$ has a NPV and a PPV for $F_{2-4}$ of 64% and 88%, respectively.

The FIB-4 values are calculated using the following formula (Sterling et al. 2006; Vallet-Pichard et al. 2007):

$$FIB4 = age[year]$$
$$\times \frac{AST[IU/L]}{\text{Platelet count}\left[10^9/L\right] \times \sqrt{ALT[IU/L]}}$$

(2)

A FIB-4 value $>3.25$ is associated with 82.1% prediction of $F_{3-4}$. A FIB-4 value $<1.45$ allows the exclusion of $F_3-F_4$ in 94.7% of HCV infected patients.

The FORNS index (Forns et al. 2002) is calculated from cholesterol, $\gamma$-glutamyl transferase level, platelets count and age, as:

$$FORNS = 7.811 - 3.131 \times ln\left(\text{Platelet count}\left[10^9/L\right]\right)$$
$$+ 0.781 \times ln(GGT[IU/L])$$
$$+ 3.467 \times ln(age[year])$$
$$- 0.014 \times cholesterol[mg/dL]$$

(3)

A FORNS score $<4.21$ has a NPV for $F_{2-4}$ of 96% (corresponding in most patients to $F_{0-1}$.

Predicted fibrosis is staged on a 0 to 4 scale. The reference predicted fibrosis level used in the statistic analysis is derived from the concordance of the biochemical noninvasive scores. This method fits an algorithm that has already been proposed and validated recently (Sebastiani et al. 2009). On the basis and according to the concordance of the biochemical noninvasive scores, it was possible to conclude:

- to mild fibrosis ($F_{0-1}$) with APRI $<0.50$, FORNS $<4.21$ and FIB-4 $<0.7$.
- to $F_2$ fibrosis with APRI $<1.0$, FORNS $>4.21$ and FIB-4 $<1.45$.
- to $F_3$ fibrosis with APRI between 0.50 and 1.50 and FIB-4 $>3.25$.
- to $F_4$ fibrosis with APRI $>2$ and FIB-4 $>3.25$.

When available (for 39 patients included in this study), the liver biopsy was taken into account to delineate the patients with mild, moderate and severe fibrosis. Among the 39 patients who underwent liver biopsy in this study, LB and concordance of surrogate blood markers agreed on the diagnosis in 35 patients (90%). Among the four patients in whom they disagreed, three of them where under ongoing antifibrosis treatment. Moreover, the final characterization of the predicted fibrosis level was blindly determined by two experienced physicians specialized in hepatology (VM, AVP, BN and SP have more than 10 years of experience.)

The noninvasive evaluation of fibrosis is more recent than the fibrosis METAVIR scoring system, but its accuracy, by comparison with the results of the liver biopsy, allows its use in France instead of liver biopsy in evaluating fibrosis in HCV-infected patients. We have previously reported the good concordance between another noninvasive marker, the Fib-4, with the results of the liver biopsy or of the Fibrotest in HCV (Vallet-Pichard et al. 2007, 2008) or hepatitis B virus (HBV) infection (Mallet et al. 2009).

In our study, the predicted fibrosis levels have been derived from the concordance of different validated biochemical markers. Besides, when liver biopsy was available (39 patients), we used all the indicators to blindly define the fibrosis level, which was discussed by two physicians.

In any case, the main aim of our study was, in those patients, the comparison of the accuracy of SSI with FS in evaluating fibrosis. Although the predicted fibrosis level is not exclusively derived from the gold standard method (LB examination), this preliminary study allows to compare both techniques with a unique reference. The reader should keep in mind that the predicted fibrosis level is derived from the blood markers values and the terminology "predicted fibrosis level"

was chosen throughout the whole article to emphasize this point.

*One-dimensional transient elastography using FS*

The FS examination is performed on the same day as the SSI examination by an experienced operator, using a commercial FS apparatus. Measurements are performed on the right lobe of the liver, through intercostal spaces with the patient lying with the right arm in maximal abduction. A 5 MHz ultrasonic transducer acquires with an ultrafast frame rate (4000 Hz) of 256 single radio-frequency signals (Sandrin et al. 2003). While ultrasonic signals are recorded, a low frequency pulse is given at the surface of the body with the front face of the transducer fixed on a vibrator. Using cross-correlation algorithm between RF lines, the shear wave displacement and the shear wave speed $v_s$ inside the liver are computed from 25 to 65 mm depth. Then, the tissue elasticity $E$ is directly derived from the propagation velocity $v_s$ and the density $\rho$ ($E = 3\rho v_s^2$). The stiffer the tissue, the faster the shear waves propagate.

*Bidimensional transient elastography using SSI*

The SSI technique has been described in detail in previous publications (Bercoff et al. 2004a, 2004b; Tanter et al. 2008; Muller et al. 2009). This article is the first clinical application of the SSI mode with a curved ultrasonic probe (C4-2 ATL, Seattle, WA, USA, central frequency 2.5 MHz, 128 elements). The conventional curved probe generates several "pushing beams" at increasing depth in the liver tissues. A pushing beam corresponds to a remote radiation force induced by a focused ultrasound beam. This radiation force creates a mechanical displacement in the focal spot of the liver tissues of the order of magnitude of a few $\mu$m. By successively focusing beams at five
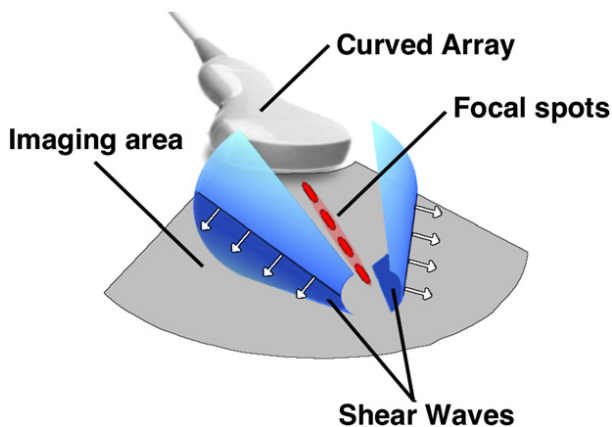


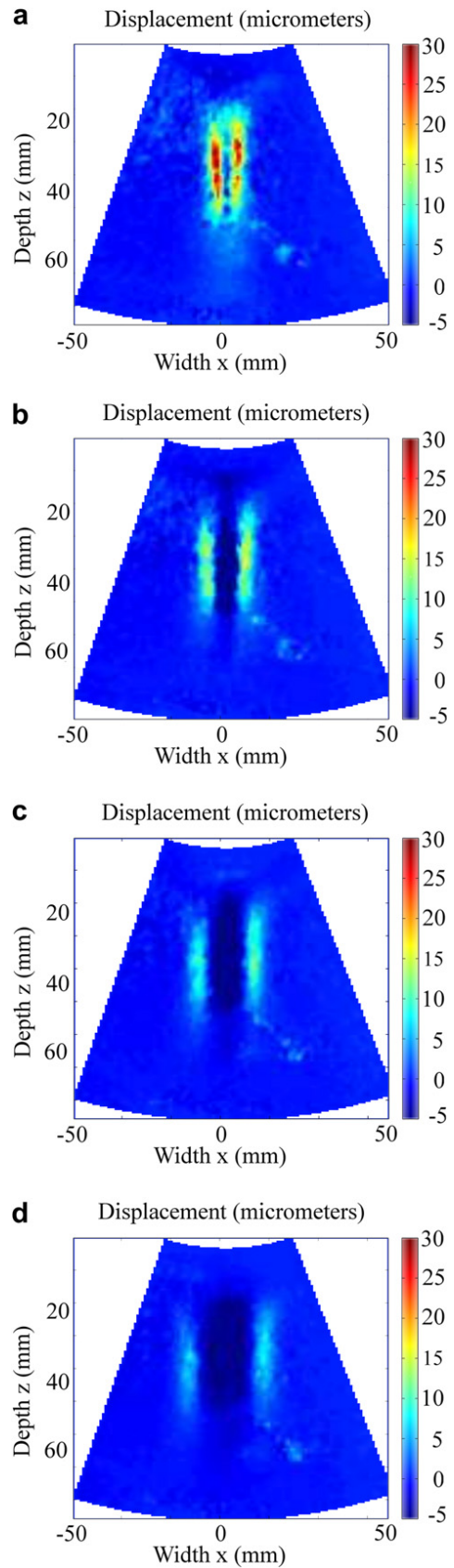Fig. 1. Generation of a conical shear wave from pushing beams at increasing depths.



Fig. 2. Displacement field at four successive times: [(a) t = 1.25 ms – (b) t = 2.0 ms – (c) t = 2.75 ms – (d) t = 3.5 ms].
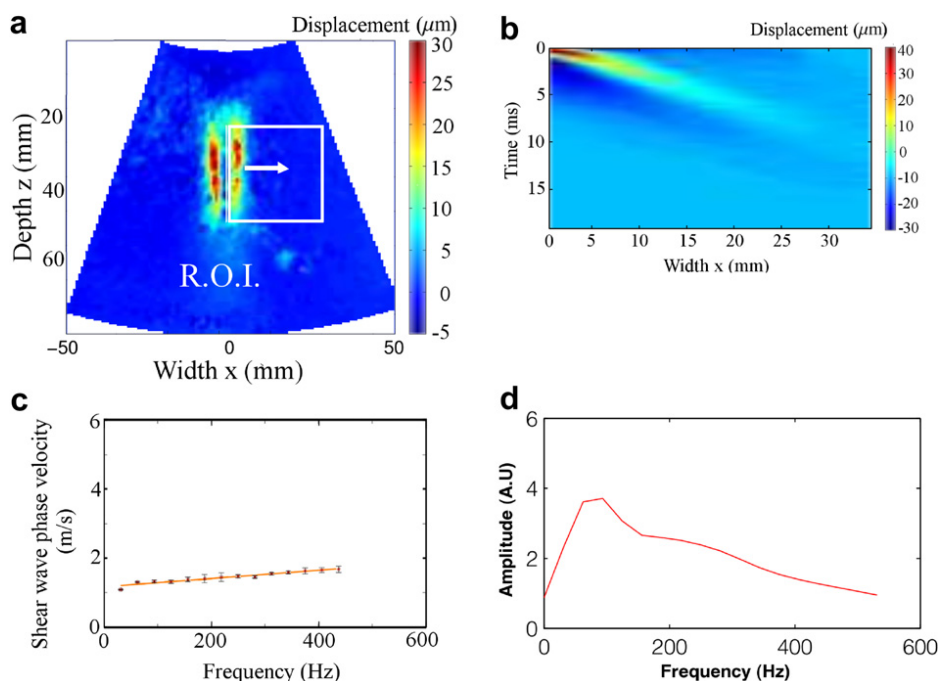
Fig. 3. (a) Region-of-interest (ROI) for the shear wave velocity dispersion calculation. (b) Space-time representation of the shear wave dispersion, derived from the tissues displacement movie (Fig. 2a–d) in the ROI. (c) Corresponding shear wave velocity dispersion, with a linear fit. (d) Corresponding spectrum.

increasing depths separated by 4.25 mm, a shear wave is generated and propagates in the tissues (Fig. 1). The depth of the first pushing beam is adjusted for each patient using a conventional B-mode image to avoid pushing in the intercostal muscle region. In the imaging plane, this shear wave front can be approximated by a planar wave front.

After this remote excitation, the ultrafast echographic device acquires at a high frame rate (4000 frames/s) in-phase/quadrature (IQ) data using the same curved ultrasonic probe. The tissues displacement field induced by the propagation of the shear waves is then derived from these IQ data (Fig. 2).

To investigate a larger region of the liver, the SSI sequence is repeated successively in three different directions (one sequence in the center of the array, one sequence at the left and one sequence at the right). The three sequences last less than 1 s of experiment. This results in a set of three propagation movies that are used to assess the shear wave velocity $v_s$ in the liver tissues using a time of flight algorithm. The livers tissues stiffness $E$ is then calculated directly from the shear wave velocity: $E = 3\rho v_s^2$. For more information on the calculation process, refer to Tanter et al. (2008).

Measurements on each patient were performed on the right lobe of the liver. The ultrasonic probe is positioned in intercostal spaces, the patient lying on his back, with the right arm raised. The probe is covered with coupling gel placed on the skin, between the rib bones. The operator positions the probe using a conventional real-time B-mode image to locate a large liver imaging area. When the target area is located, the operator launches the SSI sequence measurement. This measurement (which lasts less than 5 s on the research prototype), is reproduced five consecutive times for each patient to test the intraoperator reproducibility. The whole examination lasts less than 3 min.

*Shear wave spectroscopy and supersonic shear imaging*

Thanks to its ability to image fast and transient motion of the shear waves, SSI can provide even more refined information about the mechanical properties of tissue than just a single estimation of Young's modulus. Indeed, the commonly accepted relationship between the shear wave speed $c_s$ and Young's modulus $E$ via $c_s = \sqrt{\dfrac{E}{3\rho}}$ is only valid if soft tissues are considered as purely elastic and incompressible medium. Under such assumption, as $c_s$ does not depend on the vibration frequency, the profile of the planar shear wave generated by the supersonic source can be considered to be undistorted during propagation. This approximation of a purely elastic medium leads to the stiffness image provided in SSI by the estimation of the group speed (wave packet speed) of the shear wave.

Contrary to FS, as vibration induced by the radiation force creates a short transient excitation, the frequency bandwidth of the generated shear wave is large, typically ranging from 60 to 600 Hz (Fig. 3). Such wideband "shear wave spectroscopy" can give a refined analysis of the complex mechanical behavior of tissue. As shown in Figure 3, the shear wave dispersion law can be assessed from displacement movies in the region-of-interest.

Thus, the global elasticity imaged by SSI makes use of higher frequency content and is also influenced by the dispersive properties of the liver tissues because it averages the full mechanical response of the liver tissues over a large bandwidth. In parallel, SWS provides a refined analysis in a larger box of these dispersive properties of tissues by estimating frequency dependence of the shear wave speed.

### Statistical methods

The diagnosis performance of FS and SSI are compared by using receiver operating characteristic (ROC) curves and box-and-whisker curves on the same cohort. A patient was assessed as positive or negative according to whether the noninvasive marker value was greater than or less than to a given cutoff value, respectively. Connected with any cutoff value is the probability of a true positive (sensitivity) and the probability of a true negative (specificity). The ROC curve is a plot of sensitivity vs. (1-specificity) for all possible cutoff values. The most commonly used index of accuracy is the area under the ROC curve (AUROC), with values close to 1.0 indicating high diagnosis accuracy. Optimal cutoff values for liver stiffness were chosen to maximize the sum of sensitivity and specificity and positive and negative predictive values were computed for these cutoff values. By using these cutoff values, the agreement between FS and SSI was evaluated. Statistical analyses were performed with Matlab R2007a software (Mathworks, Natick, MA, USA) using the statistical analysis toolbox and Medcalc software (Mariakerke, Belgium).

### RESULTS

#### Liver stiffness mapping using SSI

The Young's modulus corresponding to the stiffness of the liver tissues are presented for 4 patients in Figure 4. The elasticity mapping is superimposed with the corresponding B-mode images on which the fat and muscle region are well differentiated from the liver region and the elasticity is mapped only in the liver region. Figure 4a, b, c and d show the elasticity mapping for patients who have been classified as predicted fibrosis levels F1, F2, F3 and F4, respectively.

The median elasticity derived from these maps are equal to $4.78 \pm 0.83$ kPa for the patient with F1, $10.64 \pm$



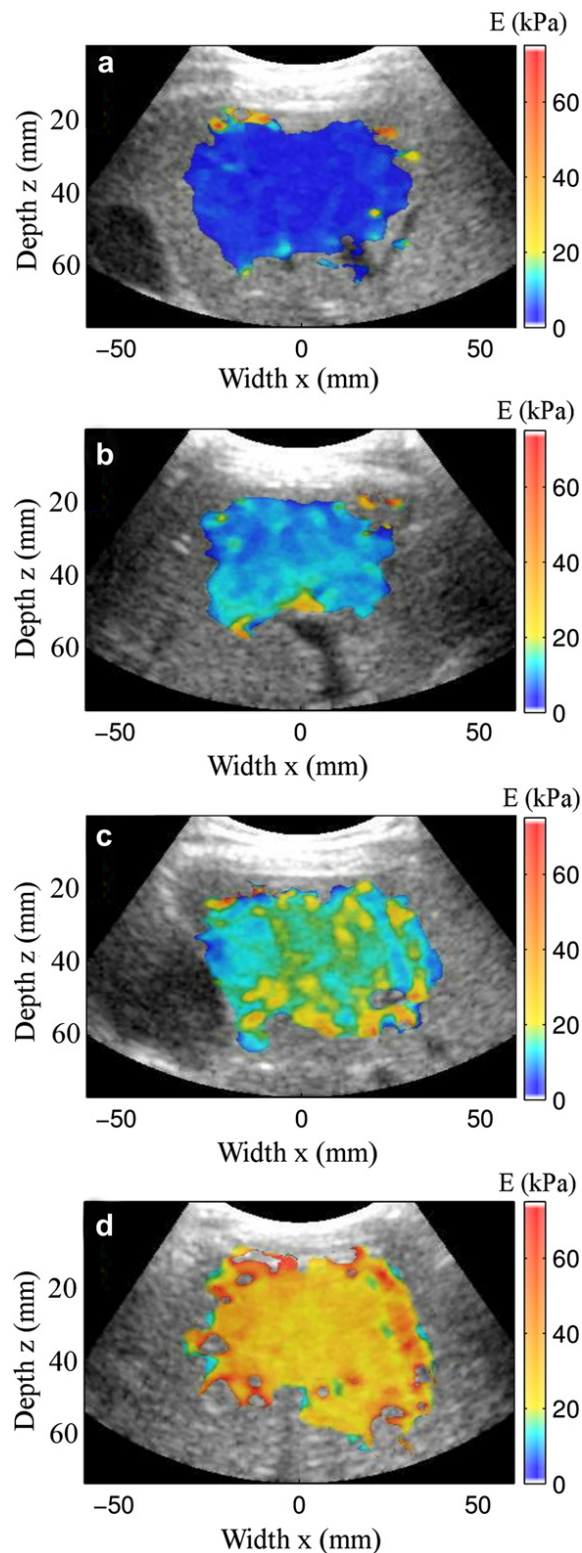Fig. 4. Bidimensional liver elasticity maps assessed using the supersonic shear imaging (SSI) technique superimposed to the corresponding B-scan. The Young's modulus representing the liver stiffness is represented in color levels. (a): patient 59 - F1. E = $4.78 \pm 0.83$ kPa (b): patient 51 - F2. E = $10.64 \pm 1.10$ kPa (c): patient 39 - F3. E = $14.52 \pm 2.20$ kPa (d): patient 22 - F4. E = $27.43 \pm 2.64$ kPa.
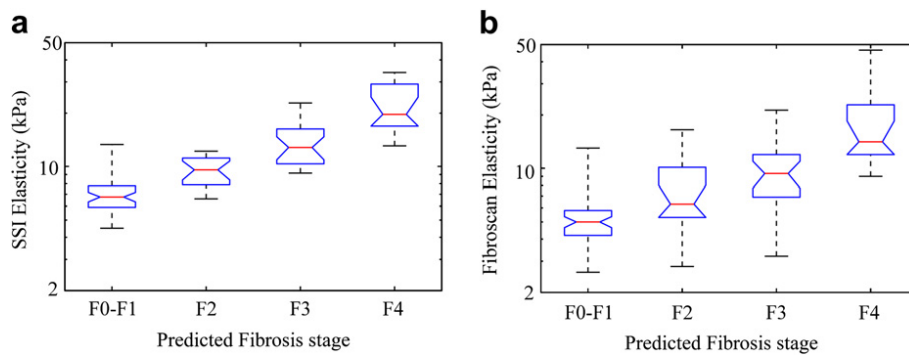
Fig. 5. Box and whisker plots of (a) supersonic shear imaging (SSI) and (b) FibroScan (FS) values for each fibrosis stage. Each box represents the interquartile range within which 50% of the elasticity values are located, around the median elasticity.

1.10 kPa for patient with F2, 14.52 ± 2.20 kPa for patient with F3 and 27.43 ± 2.64 kPa for the patient with F4. The mean surface of the region in which the global elasticity is assessed for these four patients equals to 16.39 ± 2.77 cm$^2$. The liver heterogeneities observed in 2-D maps are less likely to introduce biases in the elasticity measurement with a curved array SSI than with FS since

the global elasticity is assessed on a larger area (2-D vs. 1-D).

*Predicted liver fibrosis level evaluation: comparison between FS and SSI*

Figure 5 shows box and whisker plots of SSI elasticity values (assessed from shear wave group velocity)
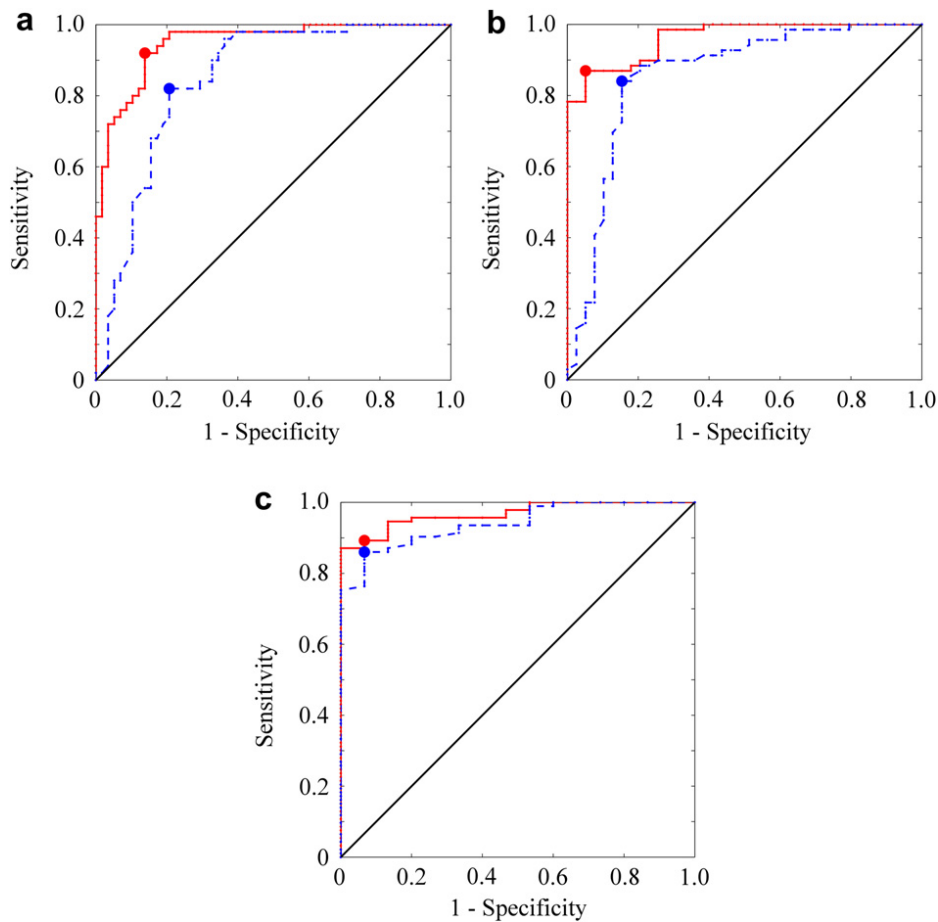


Fig. 6. ROC curves for supersonic shear imaging (SSI) (solid line) and FibroScan (FS) (dashed line) for different fibrosis thresholds: (a) F0-F1 vs. F2-F4 (*p* index:0.005), (b) F0-F2 vs. F3-F4 (*p* index:0.001) and (c) F0-F3 vs. F4 (*p* index:0.154). The most discriminant cutoff values in this study are shown for reference.

Table 1. AUROC and 95% confidence interval for SSI and FS according to METAVIR fibrosis stages

| Method | $F \geq 2$ | $F \geq 3$ | $F = 4$ |
|---|---|---|---|
| SSI | 0.95 [0.91;0.99] | 0.96 [0.92;1] | 0.97 [0.90;1] |
| FS | 0.85 [0.77;0.92] | 0.86 [0.77;0.93] | 0.94 [0.85;1] |
| FS (Castéra et al. 2005) | 0.83 [0.76;0.88] | 0.90 [0.85;0.94] | 0.95 [0.91;0.98] |
| Δ | 0.102 ± 0.0367 | 0.105 ± 0.0407 | 0.027 ± 0.0193 |
| P | 0.005 | 0.001 | 0.154 |

SSI = supersonic shear imaging; FS = FibroScan; AUROC = area under the receiver operating characteristic curve.
The results from a previous study (Castéra et al. 2005) on fibrosis staging using FS are shown for reference. Δ, the difference between AUROC for SSI and FS are also presented. The significance level $P$ of the comparison between ROC curves is also given.

and FS elasticity values for each predicted liver fibrosis level. Although the predicted fibrosis level is not exclusively derived from the gold standard method (LB examination), this preliminary study allows the comparison of both techniques with a unique reference: the predicted fibrosis level, which is derived from the blood markers values and liver biopsy, when available. The corresponding one-way analysis of variance (ANOVA) gives both a $p$ index of $<10^{-5}$. In this analysis, the liver elasticity distributions are normalized by log transformation to ensure the validity of the analysis of variance. SSI allows evaluating the patients liver fibrosis with a smaller variance than FS for all liver predicted fibrosis levels. To analyse the fibrosis evaluation performances, FS and SSI are compared by using receiver operating characteristic (ROC) curves in the following.

Figure 6 shows ROC curves comparison and the significance level $p$ for AUROC comparison using DeLong method (DeLong et al. 1988) for different degrees of predicted liver fibrosis levels. The corresponding comparison between AUROCs and confidence levels are shown in Table 1 and the most discriminant cutoff values are shown in Table 2.

Table 2. Liver stiffness cutoff values in this study and performance indicators of diagnosis accuracy (sensitivity, specificity, Youden's index and misclassification rate) for SSI and FS elasticity measurement methods

| Value | Method | $F \geq 2$ | $F \geq 3$ | $F = 4$ |
|---|---|---|---|---|
| Optimal cutoff (kPa) | SSI | 9.12 | 10.08 | 13.30 |
| | FS | 5.80 | 7.20 | 10.30 |
| Specificity at 95% of sensitivity | SSI | 0.81 | 0.75 | 0.80 |
| | FS | 0.64 | 0.49 | 0.47 |
| Sensitivity at 95% of specificity | SSI | 0.72 | 0.78 | 0.87 |
| | FS | 0.20 | 0.21 | 0.76 |
| Youden's index | SSI | 0.78 | 0.82 | 0.83 |
| | FS | 0.61 | 0.69 | 0.79 |
| Misclassification rate | SSI | 0.11 | 0.10 | 0.10 |
| | FS | 0.19 | 0.16 | 0.13 |

SSI = supersonic shear imaging; FS = FibroScan.
These cutoff values are shown as a preliminary result, as cutoff elasticity values will have to be optimized in further clinical studies relying on more patients.

As shown in Table 1, the FS examination gives worse AUROCs for each predicted fibrosis level than SSI. The AUROCs values for SSI and FS are, respectively, 0.948 and 0.846 for the diagnosis of significant fibrosis ($F \geq 2$), 0.962 and 0.857 for the diagnosis of severe fibrosis ($F \geq 3$); for the diagnosis of cirrhosis ($F = 4$), the AUROC values are 0.968 and 0.940, respectively.

Furthermore, other indicators of the performances of diagnosis tests are derived from ROC curves for SSI and FS measurements. For all predicted liver fibrosis levels, misclassification rates and Youden's index confirm the fact that the diagnosis accuracy is better using SSI than FS when comparing predicted liver fibrosis levels using noninvasive markers (and biopsy when available). For all stages of liver fibrosis, the specificity at 95% of sensitivity is higher for SSI than FS, as well as the sensitivity at 95% of specificity is higher for SSI than FS (see Table 2).

*Liver stiffness evaluation: comparison between FS and SSI*

Liver elasticity values assessed using SSI ranged from 4.50 kPa to 33.96 kPa (median 9.14 kPa, standard deviation 6.27 kPa). Liver elasticity values assessed using FS ranged from 2.60 kPa to 46.50 kPa (median 6.10 kPa, standard deviation 6.41 kPa). The liver stiffness distributions assessed by FS and SSI are presented on Figure 7 using a scatter plot (with liver stiffness distribution normalized by log transformation) and a Bland-Altman representation. This multivariate analysis shows a good correlation ($r = 0.8296$, $p < 10^{-5}$) between the elasticity values assessed by FS and SSI apparatus. Moreover, the Bland-Altman analysis shows a good agreement between the two methods, with a mean offset between SSI and FS of 2.40 kPa (standard deviation of the difference between SSI and FS: 3.61 kPa).

Figures 7 and 8 are represented to explain two important points. On one hand, FS and SSI values are not strictly identical (as shown in Fig. 7). On the other hand, SSI values contain the information provided by the FS (as shown in Fig. 8). Figure 8 is obtained by using the SWS processing on SSI data: a linear fit of the shear wave velocity dispersion curve was performed for each
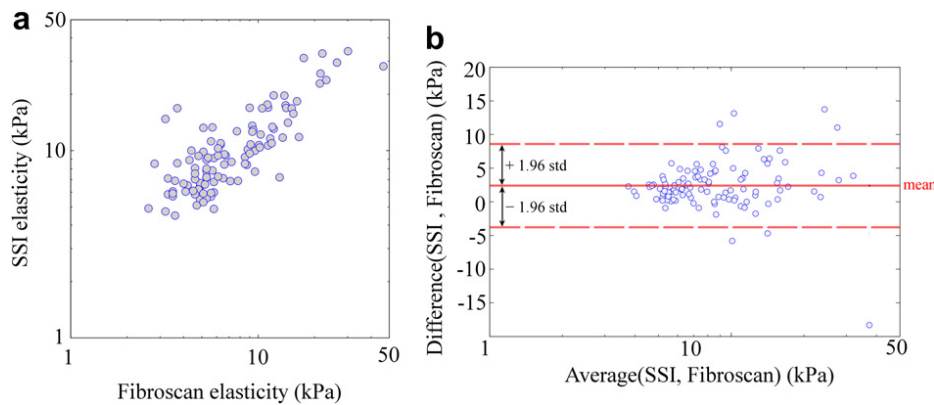
Fig. 7. (a) Scatter plot between liver stiffness distributions (normalized by log transformation) assessed by FibroScan (FS) and supersonic shear imaging (SSI) technique. (b) Bland-Altman plot between the SSI measurement and the FS measurement.

patient, from which the shear wave velocity at 50 Hz was extracted to compute the corresponding elasticity at 50 Hz. The liver stiffness distributions assessed by FS and SSI at 50 Hz (from the fit of the shear wave velocity dispersion curve at 50 Hz) are presented on Figure 8 using a scatter plot (with liver stiffness distribution normalized by log transformation) and a Bland-Altman representation. This multivariate analysis shows a good correlation ($r = 0.9742$, $p < 10^{-5}$) between the elasticity values assessed by FS and SSI apparatus at 50 Hz. Moreover, the Bland-Altman analysis shows a good agreement between the two methods when the elasticity assessed by SSI is extracted at 50 Hz, with a mean offset between SSI and FS of $-1.19$ kPa (standard deviation of the difference between SSI at 50 Hz and FS: 1.68 kPa).

*Shear wave spectroscopy*

SWS allows the assessment of the dependence of shear wave phase velocity to frequency. As a consequence, the SSI and SWS measurements take into

account the full mechanical response over a larger bandwidth. As shown in Figure 9, when the shear wave phase velocity is calculated, the dispersion slope can be derived by linear-fitting the shear wave dispersion law. The dispersion slope is a parameter that has a direct influence on the group velocity (hence the global elasticity assessed by SSI). The phase velocity and dispersion slope have been calculated using the acquired data for each patient. These measurements have been repeated five times for each patient. Then, a multiple regression analysis of shear wave velocity dispersion slope (median value over the five measurements) vs. predicted fibrosis level has been performed over the whole cohort of subjects. This analysis shows that dispersion slope measurements are not correlated significantly to predicted fibrosis level ($r = 0.1943$, $p = 0.0579$).

*Spatial heterogeneity of elasticity of liver tissues*

One point of particular interest is the spatial heterogeneity of elasticity of liver tissues ($\sigma$, kPa) and its link to
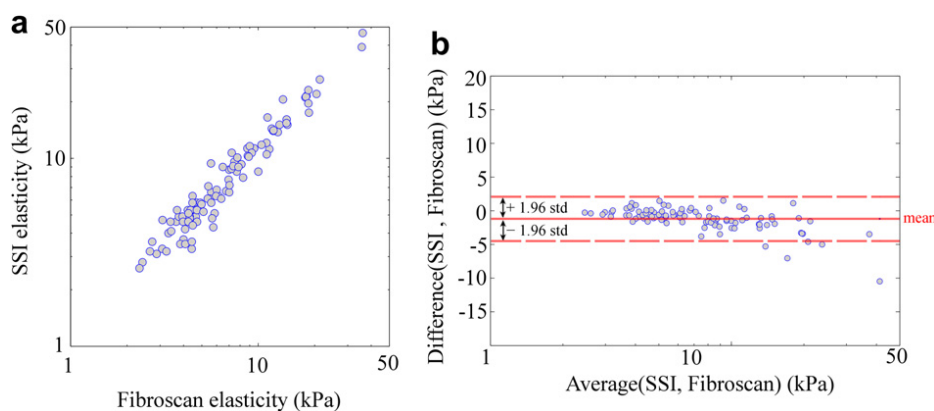


Fig. 8. (a) Scatter plot between liver stiffness distributions (normalized by log transformation) assessed by FibroScan (FS) and supersonic shear imaging (SSI) technique extracted from fit at 50 Hz. (b) Bland-Altman plot between the SSI measurements fitted at 50 Hz and the FS measurement.
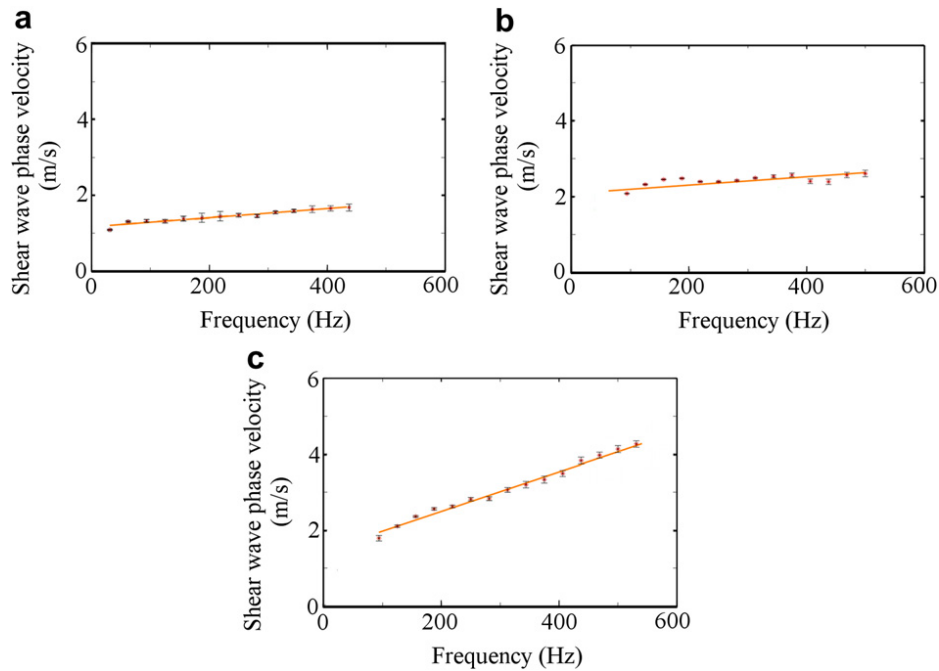
Fig. 9. Shear wave dispersion curve for (a) patient No. 111 (F1 - dispersion slope: 1.21 mm), (b) patient No. 39 (F3 - dispersion slope: 1.09 mm) and (c) patient No. 121 (F3 - dispersion slope: 5.17 mm).

the predicted fibrosis level. In our experiments, the SSI global elasticity corresponds to the median of the stiffness values mapped in the imaging plane ($E$, kPa). The standard deviation of the elasticity values corresponds to the spatial heterogeneity of liver tissues. Figure 10 shows a box and whisker representation of the spatial heterogeneity of liver tissues elasticity for each predicted fibrosis level. The corresponding one-way ANOVA analysis gives a $p$ index of $6.33 \cdot 10^{-10}$. This result suggests that the liver tissues are more and more heterogeneous when liver fibrosis increases, with a good correlation between the predicted fibrosis level and the amount of

heterogeneities in liver tissues. Interestingly, the rate of liver stiffness heterogeneity, defined as $\tau = \frac{\sigma}{E}$, also increases with the predicted fibrosis level. In this statistical study, the mean rate of liver heterogeneity equals to $\tau_{0,1} = 14.24\%$ for $F \leq 1$, $\tau_2 = 16.63\%$ for $F = 2$, $\tau_3 = 17.62\%$ for $F = 3$ and $\tau_4 = 19.29\%$ for $F = 4$.

## DISCUSSION

SSI allows assessing the elasticity of the liver tissues using the shear wave group velocity on a larger area and on a larger bandwidth than FS. This statistical study on a cohort of HCV infected patients suggests that fibrosis evaluation could be easier with SSI than FS, even if both are transient ultrasound elastography methods. This result can first be explained by the fact that SSI maps the elasticity on a larger area than FS. Thus, the liver stiffness heterogeneities are less likely to introduce biases in the SSI elasticity measurement than in FS, since they are averaged on a large spatial area. Furthermore, the FS measurement acts at 50 Hz and has a narrow frequency band measurement, whereas SSI allows a large bandwidth measurement and allows assessing the shear wave dispersion law using the SWS method. Thus, the global elasticity assessed by SSI is determined by the dispersive properties of the liver tissues that are directly linked to the elasticity of the tissues and to the predicted fibrosis level. As a consequence, the knowledge of the full mechanical response of the liver tissues allows assessing
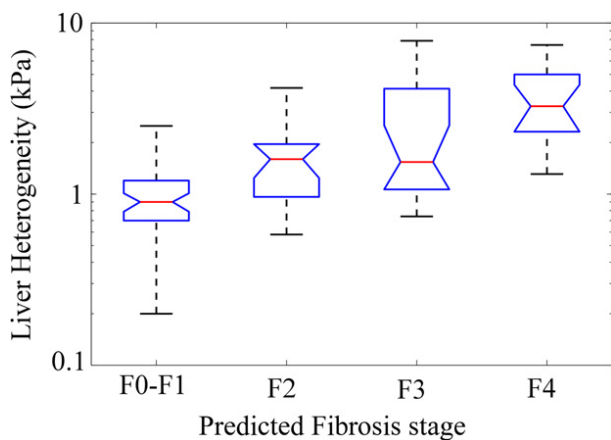


Fig. 10. Box and whisker plot of liver tissues spatial heterogeneity vs. fibrosis stage.

with more accuracy the predicted fibrosis level than the elasticity measurement at 50 Hz using FS.

Although this result has been obtained with a predicted score using both biochemical noninvasive markers and liver biopsy (when available), this preliminary study has to be confirmed with a wider analysis with more patients who underwent liver biopsy (study under progress).

Under these considerations, the comparison between ROC curves and performance indicators for SSI and FS shows that the diagnostic could be more accurate using SSI than FS. The difference between AUROCs for the detection of mild and moderate fibrosis is particularly significant ($P \leq 1\%$) and that the comparison between ROC curves for severe fibrosis is not significant ($p > 5\%$).

The comparison between the liver elasticity values assessed by SSI and FS shows a good agreement with a mean offset between SSI and FS of 2.40 kPa. This slight differences between SSI and FS are explained by the fact that the Young's modulus value (corresponding to the liver stiffness) with both SSI and FS techniques is derived from the shear group velocity. However, it is derived from the broadband (60 Hz–600 Hz) characteristic of the mechanical excitation generated using the acoustic radiation force for SSI (Muller et al. 2009; Deffieux et al. 2009), whereas FS elasticity values are assessed using an external vibrator acting at 50 Hz (Sandrin et al. 2003). Thus, the elasticity assessed by SSI corresponds to the stiffness "felt" by higher frequency vibrations. It integrates both elasticity and viscosity properties as it averages the shear wave speed over a large bandwidth.

Interestingly, extracting Young's modulus value from the linear fit of SSI data only at 50 Hz (corresponding to the vibrating frequency of FS) provides values well correlated with FS. However, as it was presented in Figure 6, SSI values by averaging shear wave speed over a large bandwidth provides a more discriminant parameter for fibrosis evaluation.

The shear wave dispersion slopes computed using SWS were not correlated significantly to predicted fibrosis level. This is an interesting result since Muller et al. (Muller et al. 2009) raised the question if the assessment of these dispersion parameters (linked to shear viscosity) would represent an added value for the diagnosis of fibrosis levels. The multiple regression analysis shows that the slope of the shear wave dispersion law is not an efficient parameter for predicted fibrosis level evaluation if taken alone. However, the large bandwidth measurement increases the diagnosis accuracy when compared with a measurement in a narrow bandwidth. The frequency dispersion of the shear wave velocity has a direct influence on the global elasticity assessed by SSI, which corresponds to an averaged value of elasticity over the whole frequency spectrum.

Moreover, it is possible that the shear wave dispersion slope alone could provide interesting information on tissue organization at the microscopic level and give information on necro-inflammatory activity. Ongoing work is investigating this assumption with a clinical study investigating SWS on livers with activity determined by an Actitest and liver biopsy (BioPredictive, Paris, France).

It has been demonstrated in this study that the rheologic behavior of the liver can be estimated locally in a large area of the liver, over a large bandwidth of mechanical excitation. The global elasticity assessed by SSI shows good diagnosis results, with high sensitivity and specificity. Dispersion curves estimated for all patients give elasticity values at 50 Hz that are in total agreement with the FS narrowband approach. Furthermore, the large spatial extent of the measurements allows SSI to be more robust to heterogeneities artefacts in the liver that we have shown to increase with predicted fibrosis level. This result on liver stiffness heterogeneity also emphasizes the fact that an efficient liver elastography should map the stiffness of the biological tissues in a large area to avoid any artefact of the tissues heterogeneities in the liver fibrosis evaluation. This confirms that SSI has a strong advantage because this method evaluates the Young's modulus in a large and deep section of the liver. Furthermore, as the spatial heterogeneity is well differentiated between liver predicted fibrosis levels, this physiologic parameter could be used to confirm the liver fibrosis evaluation assessed by SSI global elasticity measurement and improve the diagnosis efficiency without having to make another measurement.

Other noninvasive morphologic procedures for evaluation of fibrosis are in progress. The magnetic resonance elastography (MRE) procedure allows three-dimensional (3-D) quantitative mapping of the elastic properties of the liver with satisfying liver fibrosis staging (Huwart et al. 2008). However, this expensive method is time consuming and needs corrections for breathing movements (Huwart et al. 2007). Two-dimensional elastography based on ARFI also requires a long acquisition time to build the elasticity map of the liver and is sensitive to breathing displacements (Fahey et al. 2006, 2007). Although, recent studies (Palmeri et al. 2008; Yoneda et al. 2010) show encouraging results using ARFI techniques to assess liver elasticity and delineate fibrosis levels. FS, based on one-dimensional (1-D) transient elastography, is a quick estimator of the livers elasticity in a mean volume of 4 cm$^3$ and is insensitive to respiratory motion artefacts. Although the volume assessed by FS is bigger than the mean LB sample volume, the fact that FS evaluates the liver elasticity along a single A-line can lead to biases in the elasticity measurement for heterogeneous livers (Muller et al. 2009). Furthermore,

the FS technique is not considered to be accurate enough for intermediate stages of liver fibrosis (Stauber and Lackner 2007) and has the same performances as serum markers for early and intermediate stages of liver fibrosis (Castéra et al. 2005; Wong et al. 2010; Lee et al. 2010; Degos et al. 2010). Imaging techniques, such as magnetic resonance imaging, computed tomography scan, or ultrasound are also reported to be unable to determine early stages of fibrosis (Stauber and Lackner 2007; Klatt et al. 2006), although being useful for biopsy guidance. Although MRE allows 3-D measurements when SSI only allows 2-D measurements, SSI is a much less cost and time consuming as well as portable approach than MRE. Regarding ARFI, the SSI ultrafast acquisition allows to avoid complicated breathing movements corrections. At last, when compared with FS, SSI has the advantage to estimate elasticity over a large bandwidth and a bigger volume that allows a thinner discrimination at early and intermediate fibrosis stages.

## CONCLUSIONS

As a conclusion, SSI appears to be a fast, simple, reproducible and reliable method for noninvasive liver fibrosis evaluation. This method allows liver elasticity mapping in a large and deep area, preventing biases due to fibrosis heterogeneities, on contrary to FibroScan. Furthermore, the large liver area mapped using a large frequency bandwidth increases diagnosis accuracy for each predicted liver fibrosis level when compared with FibroScan, which is a 1-D measurement that acts at a 50 Hz. This suggests that SSI could be a new efficient noninvasive tool for evaluating liver fibrosis for many patients since it has good diagnosis performances for early, intermediate, as well as advanced predicted levels of fibrosis. SWS is currently under strong development for liver activity staging as a complement to SSI fibrosis evaluation.

## REFERENCES

Afdahl NH. Diagnosing fibrosis in hepatitis C: Is the pendulum swinging from biopsy to blood tests. Hepatology 2003;37:974–972.

Athanasiou A, Tardivon A, Tanter M, Sigal-Zaffrani B, Bercoff J, Deffieux T, Gennisson J-L, Fink M. Neuensschwander S. Breast lesions: Quantitative elastography with supersonic shear imaging - Preliminary results. Radiology 2010;256:297–303.

Bataller R, Brenner DA. Liver fibrosis. J Clin Invest 2005;115:209–218.

Beaugrand M. How to assess liver fibrosis and for what purpose? J Hepatol 2006;44:444–445.

Bedossa P, Dargère D, Paradis V. Sampling variability of liver fibrosis in chronic hepatitis C. Hepatology 2003;38:1449–1457.

Bedossa P, Poynard T. An algorithm for grading of activity in chronic hepatitis C. Hepatology 1996;24:289–293.

Bercoff J, Tanter M, Fink M. Sonic boom in soft materials: The elastic Cerenkov effect. Appl Phys Lett 2004a;84:2202–2204.

Bercoff J, Tanter M, Fink M. Supersonic shear imaging: A new technique for soft tissues elasticity mapping. IEEE Trans Ultrason Ferroelectr Freq Control 2004b;51:1523–1536.

Bercoff J, Tanter M, Muller M, Fink M. The role of viscosity in the impulse diffraction field of elastic waves induced by the acoustic radiation force. IEEE Trans Ultrason Ferroelectr Freq Control 2004c;51:1523–1536.

Bravo AA, Sheth SG, Chopra S. Liver biopsy. N Engl J Med 2001;344: 495–500.

Cadranel J-F, Rufat P, Degos F. Practices of liver biopsy in France: Results of a prospective nationwide survey. Hepatology 2000;32: 477–481.

Castéra L, Nègre I, Samii K, Buffet C. Pain experienced during percutaneous liver biopsy. J Hepatol 1999;30:1529–1530.

Castéra L, Vergniol J, Foucher J, le Bail B, Chanteloup E, Haaserand M, Darriet M, Couzigou P, de Lédhinghen V. Prospective comparison of transient elastography, Fibrotest, APRI and liver biopsy for the assessment of fibrosis in chronic hepatitis C. Gastroenterology 2005;128:343–350.

Chen S, Urban M, Pislaru C, Kinnick R, Zheng Y, Yao A, Greenleaf J. Shearwave dispersion ultrasound vibrometry (SDUV) for measuring tissue elasticity and viscosity. IEEE Trans Ultrason Ferroelectr Freq Control 2009;56:55–62.

Colloredo G, Guido M, Sonzogni A, Leandro G. Impact of liver biopsy size on histological evaluation of chronic viral hepatitis: The smaller the sample, the milder the disease. J Hepatol 2003;39:239–244.

Deffieux T, Montaldo G, Tanter M, Fink M. Shear wave spectroscopy for *in vivo* quantification of human soft tissues viscoelasticity. IEEE Trans Med Imaging 2009;28:313–322.

Degos F, Perez P, Roche B, Mahmoudi A, Asselineau J, Voitot H, Bedossa P, FIBROSTIC Study Group. Diagnostic accuracy of Fibro-Scan and comparison to liver fibrosis biomarkers in chronic viral hepatitis: A multicenter prospective study (the fibrostic study). J Hepatol 2010;53:1013–1021.

DeLong E, DeLong D, Clarke-Pearson D. Comparing the areas under two or more correlated receiver operating characteristic curves: A nonparametric approach. Biometrics 1988;44:837–845.

Fahey BJ, Nelson RC, Bradway DP, Hsu SJ, Dumont DM, Trahey GE. *In vivo* visualization of abdominal malignancy with acoustic radiation force elastography. Phys Med Biol 2008;53:279–293.

Fahey BJ, Palmeri ML, Trahey GE. Frame rate considerations for real-time abdominal acoustic radiation force impulse imaging. Ultrason Imaging 2006;28:193–210.

Fahey BJ, Palmeri ML, Trahey GE. The impact of physiological motion on tissue tracking during radiation force imaging. Ultrasound Med Biol 2007;33:1149–1166.

Fontana RJ, Lok ASF. Noninvasive monitoring of patients with chronic hepatitis C. Hepatology 2002;36:S57–S64.

Forns X, Ampurdanes S, Llovet JM, Aponte J, Quinto L, Martinez-Bauer E, Bruguera M, Sanchez-Tapias JM, Rodes J. Identification of chronic hepatitis C patients without hepatic fibrosis by a simple predictive model. Hepatology 2002;36:986–992.

Friedman SL. Liver biopsies, from bench to bedside. J Hepatol 2003;38: S38–S53.

Friedrich-Rust M, Ong M-F, Herrmann E, Dries V, Samaras P, Zeuzem S, Sarrazin C. Real-time elastography for noninvasive assessment of liver fibrosis in chronic viral hepatitis. Am J. Roentgenol 2007;42:758–764.

Gennisson J-L, Deffieux T, Macé E, Montaldo G, Fink M, Tanter M. Viscoelastic and anisotropic mechanical properties of *in vivo* muscle tissue assessed by supersonic shear imaging. Ultrasound Med. Biol 2010;36:789–801.

Halfon P, Bourlière M, Pénaranda G, Deydier R, Renou C, Botta-Fridlund D, Tran A, Portal I, Allemand I, Rosenthal-Allieri A, Ouzan D. Accuracy of hyaluronic acid level for predicting liver fibrosis stages in patients with hepatitis C virus. Comp Hepatol 2005;4:1–7.

Huwart L, Sempoux C, Salameh N, Jamart J, Annet L, Sinkus R, Peeters F, ter Beek LC, Horsmans Y, van Beers BE. Liver fibrosis: Noninvasive assessment with MR elastography versus aspartate aminotransferase to platelet ratio index. Radiology 2007;245: 458–466.

Huwart L, Sempoux C, Vicaut E, Salameh N, Annet L, Danse E, Peeters F, ter Beek LC, Rahier J, Sinkus R, Horsmans Y, van

Beers BE. Magnetic resonance elastography for the noninvasive staging of liver fibrosis. Gastroenterology 2008;135:32–40.

Imbert-Bismut F, Ratziu V, Pieroni L, Charlotte F, Benhamou Y, Poynard T. Biochemical markers of liver fibrosis in patients with hepatitis C virus infection: A prospective study. Lancet 2001;357: 1069–1075.

Klatt D, Asbach P, Rump J, Papazoglou S, Somasundaram R, Modrow J, Braun J, Sack I. *In vivo* determination of hepatic stiffness using steady state free precession magnetic resonance elastography. Invest Radiol 2006;42:841–848.

Lackner C, Struber G, Liegl B, Leibl S, Ofner P, Bankuti C, Bauer B, Stauber RE. Comparison and validation of simple noninvasive tests for prediction of fibrosis in chronic hepatitis C. Hepatology 2005;41: 1376–1382.

Lee MH, Cheong JY, Um SH, Seo YS, Kim DJ, Hwang SG, Yang JM, Han K-H, Cho SW. Comparison of surrogate serum markers and transient elastography (FibroScan) for assessing cirrhosis in patients with chronic viral hepatitis. Digest Dis Sci 2010;55:3552–3560.

Maharaj B, Maharaj RJ, Leary WP, Cooppan RM, Naran AD, Pirie D, Pudifin DJ. Sampling variability and its influence on the diagnostic yield of percutaneous needle biopsy of the liver. Lancet 1986;39: 523–525.

Mallet V, Dhalluin-Venier V, Roussin C, Bourliere M, Pettinelli ME, Giry C, Vallet-Pichard A, Fontaine H, Pol S. The accuracy of the FIB-4 index for the diagnosis of mild fibrosis in chronic hepatitis B. Aliment Pharmacol Ther 2009;29:409–415.

McAleavey S, Collins E, Kelly J, Elegbe E, Menon M. Validation of smurf estimation of shear modulus in hydrogels. Ultrason Imaging 2009;31:131–150.

Muller M, Gennisson J-L, Deffieux T, Tanter M, Fink M. Quantitative viscoelasticity mapping of human liver using supersonic shear imaging: Preliminary *in vivo* feasibility study. Ultrasound Med Biol 2009;35:219–229.

Muthupillai R, Lomas DJ, Rossman PJ, Greenleaf JF, Manduca A, Ehman RL. Magnetic resonance elastography by direct visualization of propagating acoustic strain waves. Science 1995;269:1854–1857.

Ono E, Shiratori Y, Okudaira T, Imamura M, Teratani T, Kanai F, Kato N, Yoshida H, Shiina S, Omata M. Platelet count reflects stage of chronic hepatitis C. Hepatol Res 1999;15:192–200.

Ophir J, Cespedesa I, Ponnekantia H, Yazdi Y, Li X. Elastography: A quantitative method for imaging the elasticity of biological tissues. Ultrason Imaging 1991;13:111–134.

Palmeri M, Wang M, Dahl J, Frinkley K, Nightingale K. Quantifying hepatic shear modulus *in vivo* using acoustic radiation force. Ultrasound Med Biol 2008;34:546–558.

Parkes J, Guha IN, Roderick P, Rosenberg W. Performance of serum marker panels for liver fibrosis in chronic hepatitis C. J Hepatol 2006;44:462–474.

Pinzani M, Rombouts K, Colagrande S. Fibrosis in chronic liver diseases: Diagnosis and management. J Hepatol 2005;42:S22–S36.

Regev A, Berho M, Jeffers LJ, Milikowski C, Molina EG, Pyrsopoulos NT, Feng Z-Z, Reddy K, Schiff ER. Sampling error and intraobserver variation in liver biopsy in patients with chronic HCV infection. Am J Gastroenterolo 2002;97:2614–2618.

Sandrin L, Fourquet B, Hasquenoph J-M, Yon S, Fournier C, Mal F, Christidis C, Ziol M, Poulet B, Kazemi F, Beaugrand M, Palau R. Transient elastography: A new noninvasive method for assessment of hepatic fibrosis. Ultrasound Med Biol 2003;29:1705–1713.

Sarvazyan AP, Rudenko OV, Swanson SD, Fowlkes J, Emelianov SY. Shear wave elasticity imaging: A new ultrasonic technology of medical diagnostics–Ultrasonic imaging of tissue strain and elastic modulus *in vivo*. Ultrasound Med Biol 1998;24:1419–1435.

Sebastiani G, Halfon P, Castéra L, Pol S, Thomas D, Mangia A, Marco VD, Pirisi M, Voiculescu M, Guido M, Bourliere M, Noventa F, Alberti A. SAFE biopsy: A validated method for large-scale staging of liver fibrosis in chronic hepatitis C. Hepatology 2009;49:1821–1827.

Stauber RE, Lackner C. Noninvasive diagnosis of hepatic fibrosis in chronic hepatitis C. World J Gastroenterol 2007;13:4287–4294.

Sterling RK, Lissen E, Clumeck N, Sola R, Correa MC, Montaner J, Sulkowski MS, Torriani FJ, Dieterich DT, Thomas DL, Messinger D, Nelson M. Development of a simple noninvasive index to predict significant fibrosis in patients with HIV/HCV coinfection. Hepatology 2006;43:1317–1325.

Tanter M, Bercoff J, Athanasiou A, Deffieux T, Gennisson J-L, Montaldo G, Muller M, Tardivon A, Fink M. Quantitative assessment of breast lesion viscoelasticity: Initial clinical results using supersonic shear imaging. Ultrasound Med Biol 2008;34: 1373–1386.

Tanter M, Touboul D, Gennisson J-L, Bercoff J, Fink M. High resolution quantitative imaging of cornea elasticity using supersonic shear imaging. IEEE Trans Med Imaging 2009;28:1881–1893.

Taylor L, Porter B, Rubens D, Parker K. Three-dimensional sonoelastography: Principles and practices. Phys Med Biol 2000;45: 1477–1494.

The French METAVIR Cooperative Study Group. Intraobserver and interobserver variations in liver biopsy interpretation in patients with chronic hepatitis C. Hepatology 1994;20:15–20.

Trinchet J- C. Clinical use of serum markers of fibrosis in chronic hepatitis. J Hepatol 1995;22:89–95.

Vallet-Pichard A, Mallet V, Nalpas B, Verkarre V, Nalpas A, Dhalluin-Venier V, Fontaine H, Pol S. FIB-4: An inexpensive and accurate marker of fibrosis in HCV infection. comparison with liver biopsy and FibroTest. Hepatology 2007;46:32–36.

Vallet-Pichard A, Mallet V, Pol S. Predictive value of FIB-4 versus fibrotest, APRI, FIBROINDEX and FORNS to noninvasively estimate fibrosis in hepatitis C. Hepatology 2008;47:763.

Wai C-T, Greenson JK, Fontana RJ, Kalbfleisch JD, Marrero JA, Conjeevaram HS, Lok AS. A simple noninvasive index can predict both significant fibrosis and cirrhosis in patients with chronic hepatitis C. Hepatology 2003;22:518–526.

Wong V, Vergniol J, Wong G, Foucher J, Chan H, Bail BL, Choi P, Kowo M, Chan A, Merrouche W, Sung J, de Ledinghen V. Diagnosis of fibrosis and cirrhosis using liver stiffness measurement in nonalcoholic fatty liver disease. Hepatology 2010;51:454–462.

World Health Organization 2004. The world health report 2004-Changing history.

Yeh W-C, Li P-C, Jeng Y-M, Hsu H-C, Kuo P-L, Li M-L, Yang P-M, Lee PH. Elastic modulus measurements of human liver and correlation with pathology. Ultrasound Med Biol 2002;28:467–474.

Yoneda M, Suzuki K, Kato S, Fujita K, Nozaki Y, Hosono K, Saito S, Nakajima A. Nonalcoholic fatty liver disease: Us-based acoustic radiation force impulse elastography. Radiology 2010;256:640–647.

Ziol M, Handra-Luca A, Kettaneh A, Christidis C, Mal F, Kazemi F, de Ledinghen V, Marcellin P, Dhumaux D, Trinchet J-C, Beaugrand M. Noninvasive assessment of liver fibrosis by measurement of stiffness in patients with chronic hepatitis C. Hepatology 2005;41:48–57.